Journal of Alloys and Compounds 515 (2012) 119–122

Contents lists available at SciVerse ScienceDirect

Journal of Alloys and Compounds

journal homepage: www.elsevier.com/locate/jallcom

Preparation and structural properties of nonlinear optical borates $K_{2(1-x)}Rb_{2x}Al_2B_2O_7$, $0 < x < 0.75$

V.V. Atuchin[a,*], B.G. Bazarov[b], T.A. Gavrilova[c], V.G. Grossman[b], M.S. Molokeev[d], Zh.G. Bazarova[b]

[a] Laboratory of Optical Materials and Structures, Institute of Semiconductor Physics, SB RAS, Novosibirsk 90, 630090, Russia
[b] Laboratory of Oxide Systems, Baikal Institute of Nature Management, SB RAS, Ulan-Ude 47, 670047, Russia
[c] Laboratory of Nanodiagnostics and Nanolithography, Institute of Semiconductor Physics, SB RAS, Novosibirsk 630090, Russia
[d] Laboratory of Crystal Physics, Institute of Physics, SB RAS, Krasnoyarsk 660036, Russia

ARTICLE INFO

Article history:
Received 20 September 2011
Received in revised form
23 November 2011
Accepted 23 November 2011
Available online 2 December 2011

Keywords:
$KRbAl_2B_2O_7$
Solid solution
Crystal structure
NLO properties

ABSTRACT

The structures of $K_{2(1-x)}Rb_{2x}Al_2B_2O_7$, $x = 0.25, 0.5, 0.75$, have been determined in space group $P321$ through Rietveld analysis of X-ray powder diffraction data. The solubility limit in $K_{2(1-x)}Rb_{2x}Al_2B_2O_7$ crystals has been estimated as $x \sim 0.83$–0.9. Nonlinear optical properties of $KRbAl_2B_2O_7$ have been verified by powder Kurtz–Perry method. Mechanisms of structural parameter variation in $K_2Al_2B_2O_7$ crystal family have been discussed.

1. Introduction

The nonlinear optical borate crystals are the basic materials of modern high-power laser systems because of appropriate nonlinear optical (NLO) coefficients, reasonable birefringence, wide transparency window including visible and UV ranges and high optical damage thresholds [1,2]. Trigonal potassium aluminum borate $K_2Al_2B_2O_7$ (KABO), space group $P321$, was discovered in ternary system K_2O–Al_2O_3–B_2O_3 [3,4]. KABO possesses a good chemical stability, reasonable NLO properties, optical transparency in UV range up to ~180 nm and the birefringence as high as $\Delta n \sim -0.08$ providing wide range lightwave phase-matching. A technology of optical quality cm^3-size KABO crystal growth was developed and the effective frequency conversion in UV spectral range was demonstrated in several experiments [5–8].

The structural and optical properties of complex NLO crystals can be tuned by doping that results in solid solution formation [9,10]. However, to have a wide solid solution range without drastic defect generation and optical quality degradation, it is desirable for the end parent crystals to be isostructural [11–15]. As to KABO, a search for structural analogs was implemented in the past because the isovalent element substitution seems to be possible in potassium or aluminum sublattices. As it was found, the Al^{3+} ions in KABO structure can be substituted by Fe^{3+} ions with the formation of $K_2Fe_2B_2O_7$, space group $P321$, showing reasonable NLO properties [16]. Regrettably, within the possible parent compounds $A_2Al_2B_2O_7$ (A = Na, K, Rb) the noncentrosymmetric structure is known only for KABO. The structure with a center of inversion was found for $Na_2Al_2B_2O_7$, space group $P\text{-}31c$ [17], and, respectively, only a limited homogeneity range was obtained for solid solution $K_{2(1-x)}Na_{2x}Al_2B_2O_7$, $0 \le x < 0.6$ [18,19]. The $Rb_2Al_2B_2O_7$ (RABO), space group $P2_1/c$, $a = 8.901(2)$, $b = 7.539(1)$, $c = 11.905(2)$, $\beta = 103.97(1)^\circ$, $V = 775.3(2)$ Å^3, $Z = 4$ also possesses a center of inversion [20]. Thus, it may be reasonably supposed that the isovalent substitution of Rb for K in KABO structure could result in the limited range solid solution $K_{2(1-x)}Rb_{2x}Al_2B_2O_7$. Phase transition $P321 \leftrightarrow P2_1/c$ is presumed to be at high rubidium content because of similar effective radii of K^+ and Rb^+ ions in oxides [21]. Thus, the present study is aimed at the evaluation of the quasi-binary system $K_2Al_2B_2O_7$–$Rb_2Al_2B_2O_7$ and the estimation of the solid solution range of KABO structure. To this end, a set of compounds $K_{2(1-x)}Rb_{2x}Al_2B_2O_7$ was prepared by solid state synthesis and the structural parameters were evaluated as a function of composition by Rietveld analysis.

2. Experimental

Polycrystalline $K_{2(1-x)}Rb_{2x}Al_2B_2O_7$ samples were prepared by solid-state reaction for $x = 0.25, 0.5, 0.75, 0.9$ using a mixture of pure $Al(NO_3)_3 \cdot 9H_2O$ (pure), H_3BO_3

* Corresponding author. Tel.: +7 383 3308889; fax: +7 383 3332771.
E-mail address: atuchin@thermo.isp.nsc.ru (V.V. Atuchin).

0925-8388/$ – see front matter © 2011 Elsevier B.V. All rights reserved.
doi:10.1016/j.jallcom.2011.11.115

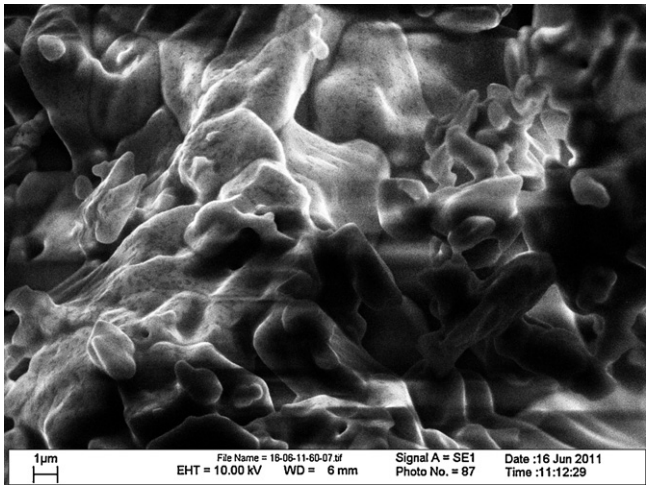

Fig. 1. SEM image of $KRbAl_2B_2O_7$ formed by solid state synthesis.

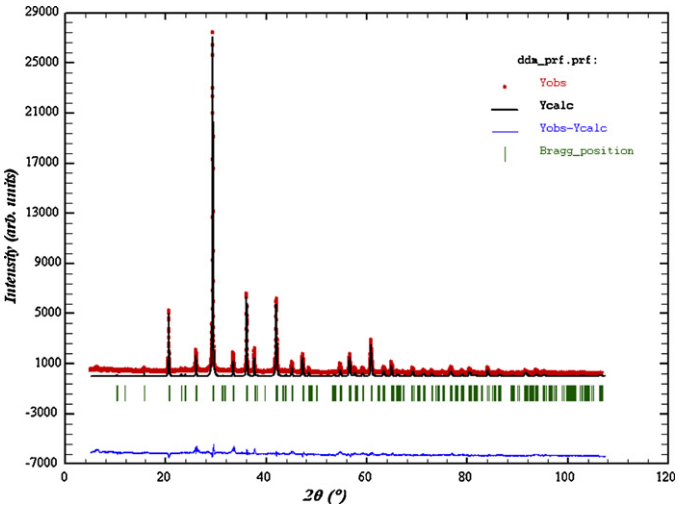

Fig. 2. X-ray diffraction patterns recorded and calculated for $KRbAl_2B_2O_7$ at room temperature.

(chemically pure grade), K_2CO_3 (chemically pure grade), Rb_2CO_3 (chemically pure grade) in stoichiometric ratio as the starting materials. Initially, to minimize the content of water captured from the environment, the carbonates were annealed at 300 °C in the dry air flow. Phase purity of annealed carbonates was verified with XRD analysis. The stoichiometric charges with compositions of $K_{2(1-x)}Rb_{2x}Al_2B_2O_7$, $x = 0.25, 0.5, 0.75, 0.9$ were prepared in a dry glove-box under nitrogen atmosphere. The charges were being fired at 120 °C for 1 h, 150 °C – 1 h, 220 °C – 3 h, 300 °C – 5 h, 350 °C – 15 h initially, then chaffed and heated next time at 400 °C for 7 h, 450 °C – 40 h, 520 °C – 40 h, 600 °C – 48 h, 700 °C – 20 h, 800 °C – 45 h, and 850 °C – 25 h. The final powder products of high temperature synthesis were of pure white color. Micromorphology of the samples was observed by SEM using LEO 1430 device.

The diffraction data for Rietveld analysis were collected at room temperature (25 °C) with a Bruker D8 ADVANCE powder diffractometer in the Bragg-Brentano geometry and linear Vantec detector. The operating parameters were: *CuKα* radiation, step size 0.016°, counting time 0.6 s per step. The data were collected over the range of 2θ: 5–107°. The peak positions were determined with EVA program, available in the PC software package DIFFRAC-PLUS supplied from Bruker. The X-ray patterns of the title compound were indexed using ITO program [22]. Almost all the observed reflections were consistent with the hexagonal symmetry, except for several small peaks that could not be definitely assigned. The borates $K_{2(1-x)}Rb_{2x}Al_2B_2O_7$ were isostructural to KABO; so, we use space group *P*321 and atom coordinates earlier reported for KABO as initial parameters for the refinement [23]. All refinements and data processing have been performed by DDM program [24]. The Pearson VII function was used to simulate the peak profiles. The acentric crystal structure of KRABO is confirmed by powder Kurtz–Perry method [25]. Noticeable second harmonic generation (SHG) signal is detected under pulse pumping at $\lambda = 1.06$ μm.

3. Results and discussion

In Fig. 1 the micromorphology is shown for the sample with nominal composition $KRbAl_2B_2O_7$ (KRABO). The irregular particles with characteristic dimensions of ~1–10 μm are found. It is evident that temperature–time conditions selected for the high temperature treatments were sufficient for the borate grains to be well coalesced due to diffusion intergrowth.

The refinement of structures of solutions $K_{2(1-x)}Rb_{2x}Al_2B_2O_7$, $x = 0.25$, 0.5, 0.75, with *P*321 space group was stable and led to minimal *R*-factors. As an example, the refinement of KRABO is considered in details. The experimental and theoretical X-ray diffraction patterns obtained for KRABO are shown in Fig. 2. A good relation between experimental and theoretical curves is evident. The results of structure determination of other compositions can be found in Supplementary Materials. The dependence of structural parameters of solid solutions $K_{2(1-x)}Rb_{2x}Al_2B_2O_7$ on *x* parameter is shown in Fig. 3. The rubidium content increase results in the quasi-linear increase of cell parameters and cell volume. There was no KABO-type structure detected for a powder sample with nominal composition $x = 0.9$ and the solubility limit in $K_{2(1-x)}Rb_{2x}Al_2B_2O_7$ crystals can be estimated as $x \sim 0.83$–0.9 at ambient conditions.

The parameters of the refinement and atom coordinates of KRABO are shown in Tables 1 and 2, respectively. Thermal parameters of Al, O and B were fixed. The main inter-atom bond lengths are reported in Table 3. The crystal structure of KRABO is shown in Fig. 4 [26]. The structure is formed by a framework of corner-linked AlO_4 tetrahedrons and BO_3 triangles. Rb and K

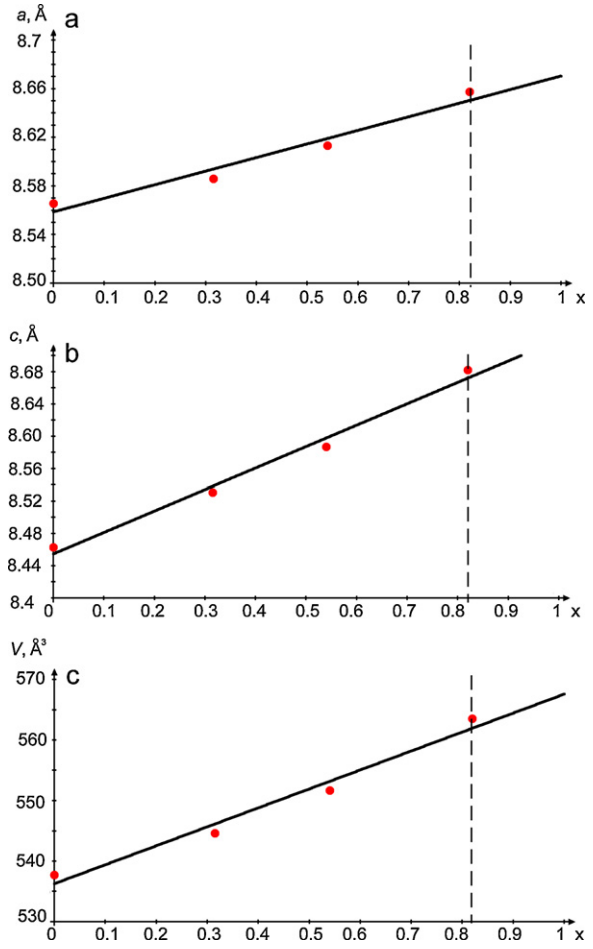

Fig. 3. Dependences of cell parameters (a) *a*, (b) *c*, and (c) cell volume *V* on composition in solid solutions $K_{2(1-x)}Rb_{2x}Al_2B_2O_7$.

Table 1
The main parameters of processing and refinement of $KRbAl_2B_2O_7$.

Space group	*P*321
a, Å	8.6131(1)
c, Å	8.5870(2)
V, Å^3	551.68(2)
2θ-interval range,°	5–107
Number of reflexions	546
Number of refinement parameters	26
R_B	6.39%
R_{DDM}	13.32%

Table 2
Atom coordinates, isotropic thermal parameters (B_{iso}) and occupancies of atom positions (*p*) in the structure of $KRbAl_2B_2O_7$ at room temperature.

Atom	*p*	*X*	*Y*	*Z*	B_{iso}, Å^2
Rb1	0.57(3)	0.316(3)	0	0	1.8(2)
K1	0.43(3)	0.316(3)	0	0	1.8(2)
Rb2	0.52(3)	0.350(3)	0	1/2	3.7(3)
K2	0.48(3)	0.350(3)	0	1/2	3.7(3)
Al1	1.0	0	0	0.282(4)	1.0
Al2	1.0	1/3	2/3	0.176(4)	1.0
Al3	1.0	2/3	1/3	0.235(4)	1.0
O1	1.0	0.161(7)	0.213(9)	0.231(4)	1.0
O2	1.0	0.383(7)	0.522(8)	0.272(4)	1.0
O3	1.0	0.450(9)	0.274(8)	0.287(4)	1.0
O4	1.0	0	0	1/2	1.0
O5	1.0	2/3	1/3	0.033(4)	1.0
B	1.0	0.33(3)	0.34(2)	0.24(1)	1.0

Table 3
Interatomic distances in the$KRbAl_2B_2O_7$ structure at room temperature.

Bond	Length, Å	Bond	Length, Å
Rb1(K1)–O1[a]	2.81(7)	Al2–O2[f]	1.72(5)
Rb1(K1)–O1[b]	2.81(4)	Al2–O2[e]	1.72(5)
Rb1(K1)–O5	2.96(1)	Al2–O2	1.72(5)
Rb1(K1)–O5[c]	2.96(1)	Al2–O5[g]	1.79(5)
Rb2(K2)–O3	2.76(5)	Al3–O3[e]	1.73(9)
Rb2(K2)–O3[c]	2.76(4)	Al3–O3[f]	1.73(5)
Rb2(K2)–O2[d]	2.79(4)	Al3–O3	1.73(8)
Rb2(K2)–O2[e]	2.79(6)	Al3–O5	1.73(5)
Al1–O1[e]	1.71(6)	B–O1	1.3(2)
Al1–O1[f]	1.71(6)	B–O2	1.4(2)
Al1–O1	1.71(6)	B–O3	1.4(2)
Al1–O4	1.87(3)		

[a] *y*, *x*, −*z*.
[b] *y* − *x*, −*x*, *z*.
[c] *x* − *y*, −*y*, −*z*.
[d] −*x*, *y* − *x*, −*z*.
[e] −*y*, *x* − *y*, *z*.
[f] *y* − *x*, −*x*, *z*.
[g] *x* − *y*, −*y*, −*z*.

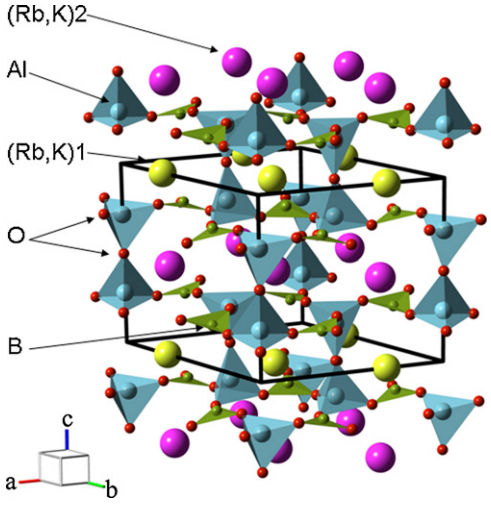

Fig. 4. The crystal structure of $KRbAl_2B_2O_7$ at room temperature.

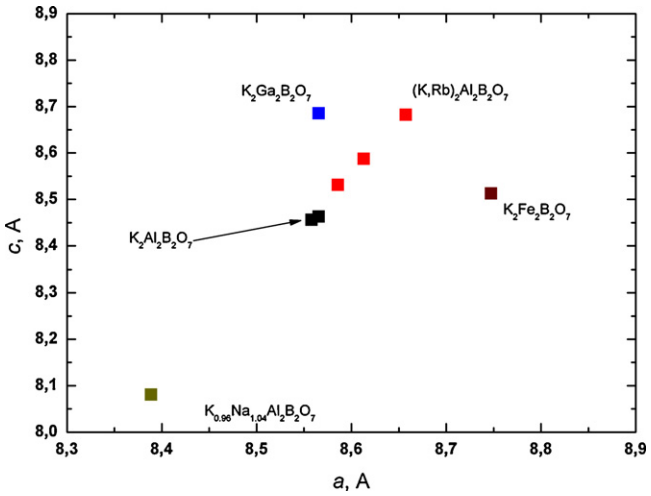

Fig. 5. Crystals with KABO-type structure on the *a*–*c* plane.

atoms have the same coordinates and the sum of the partial occupancies is equal to 1. The refinement of the partial occupancies of K1 and K2 positions by Rb and K atoms leads to formula $(K_{0.57(3)}Rb_{0.43(3)})(K_{0.52(3)}Rb_{0.48(3)})Al_2B_2O_7$. So, there is no significant preference for the incorporation of Rb atoms into K1 and K2 positions in the KRABO crystal lattice. However, some decrease of rubidium total content is detectable in reference to the initial charge composition. It is interesting to compare the geometry of AlO_4 tetrahedrons in KABO and KRABO. In both structures the AlO_4 pyramids have an equilateral triangle as a base and one specific Al–O distance along the polar crystallographic axis. In KABO structure, this apex Al–O distance is shorter than other three Al–O distances in the AlO_4 pyramids. Such a compression of AlO_4 tetrahedrons is found for all the three Al positions in KABO structure. The continuous increase of the apex Al–O distances is observed with Rb doping in $K_{2(1-x)}Rb_{2x}Al_2B_2O_7$ crystals and the AlO_4 tetrahedrons become elongated in the polar crystallographic direction. This mechanism provides a drastic increase of cell parameter *c* with Rb-doping level increase. The contraction of the base triangles of the AlO_4 tetrahedrons with Rb doping, however, is not resulted in cell parameter *a* decrease because the free space appeared is occupied by big Rb^+ ions.

In Fig. 5 all the presently known KABO-type crystals are plotted at the *a*–*c* plane that permits us to estimate the stability of KABO structure on atom substitution and doping [16–18,27,28]. Giant variation of cell parameters *a* (~4.2%) and *c* (7%) is possible over a field of KABO-type structures. As it appears, so large ranges of the structural parameters variation are provided by the flexibility of KABO structure where all the comparatively rigid atomic constructions of AO_4 (A = Al, Ga, Fe) and BO_3 are corner-linked with a wide-range rotation freedom. It should be pointed, that wide range tuning of the structural parameters is possible in solid solutions $K_{2(1-x)}E_{2x}Al_2B_2O_7$ (E = Na, Rb). This gives a promise for a wide range tuning of linear optical parameters of the crystals because ionic refractions of Na^+, K^+ and Rb^+ ions are noticeably different [29,30].

4. Conclusions

The wide range solid solutions with KABO structure are found in the $K_2Al_2B_2O_7$–$Rb_2Al_2B_2O_7$ system. The upper limit of rubidium solubility is as high as $x \sim 0.83$–0.90 under ambient conditions. The $K_{2(1-x)}Rb_{2x}Al_2B_2O_7$ crystals possess nonlinear optical properties and can be used for frequency conversion. Isovalent substitution of Rb^+ ions for K^+ ions in KABO lattice results in a strong increase of structural parameters *a* and *c* and the cell volume.

The KABO-type structure is very flexible and accepts a giant variation of the structural parameters *a* and *c* and, respectively, wide range solutions could be supposed in $K_2Al_2B_2O_7$–$K_2Ga_2B_2O_7$ and $K_2Al_2B_2O_7$–$K_2Fe_2B_2O_7$ systems.

Acknowledgements

This study was supported by SB RAS (Grant 34) and RFBR Grants 11-02-90706-mob_st and 11-03-00867a.

Appendix A. Supplementary data

Supplementary data associated with this article can be found, in the online version, at doi:10.1016/j.jallcom.2011.11.115.

References

[1] Z.-G. Hu, M. Yoshimura, Y. Mori, T. Sasaki, J. Cryst. Growth 275 (2005) 232–239.
[2] C. Chen, Z. Lin, Z. Wang, Appl. Phys. B 80 (2005) 1–25.
[3] Z.-G. Hu, T. Higashiyama, M. Yoshimura, Y.K. Yap, Y. Mori, T. Sasaki, Jpn. J. Appl. Phys. 37 (1998) L1093–L1094.
[4] N. Ye, W. Zeng, J. Jiang, B. Wu, C. Chen, B. Feng, X. Zhang, J. Opt. Soc. Am. 17 (5) (2000) 764–768.
[5] Z.-G. Hu, M. Yoshimura, Y. Mori, T. Sasaki, K. Kato, Opt. Mater. 23 (2003) 353–356.
[6] C. Zhang, J. Wang, X. Cheng, X. Hu, H. Jiang, Y. Liu, C. Chen, Opt. Mater. 23 (2003) 357–362.
[7] N. Umemura, M. Ando, K. Suzuki, E. Takaoka, K. Kato, Z.-G. Hu, M. Yoshimura, Y. Mori, T. Sasaki, Appl. Opt. 42 (15) (2003) 2716–2719.
[8] P. Kumbhakar, T. Kobayashi, J. Appl. Phys. 94 (3) (2003) 1329–1338.
[9] J.J. Huang, G.J. Ji, T. Shen, Yu.M. Andreev, A.V. Shaiduko, G.V. Lanskii, U. Chatterjee, J. Opt. Soc. Am. B 24 (9) (2007) 2443–2453.
[10] J.J. Huang, W. Gao, T. Shen, B.L. Mao, Yu.M. Andreev, A.V. Shaiduko, G.V. Lanskii, U. Chatterjee, V.V. Atuchin, J. Opt. Soc. Am. B 24 (12) (2007) 3081–3090.
[11] S.J. Crennell, A.K. Cheetham, J.A. Kaduk, R.H. Jarman, J. Mater. Chem. 2 (8) (1992) 785–792.
[12] I. Savatinova, I. Savova, E. Liarocapis, C.C. Ziling, V.V. Atuchin, M.N. Armenise, V.M.N. Passaro, J. Phys. D: Appl. Phys. 31 (1998) 1667–1672.
[13] I.E. Kalabin, D.I. Shevtsov, I.S. Azanova, I.F. Taysin, V.V. Atuchin, A.B. Volyntsev, A.N. Shilov, J. Phys. D: Appl. Phys. 37 (2004) 1829–1833.
[14] Yu.M. Andreev, V.V. Atuchin, G.V. Lanskii, N.V. Pervukhina, V.V. Popov, N.C. Trocenco, Solid State Sci. 7 (2005) 1188–1193.
[15] M.V. Shevchuk, V.V. Atuchin, A.V. Kityk, A.O. Fedorchuk, Y.E. Romanyuk, S. Całus, O.M. Yurchenko, O.V. Parasyuk, J. Cryst. Growth 318 (2011) 708–712.
[16] Y. Wang, R.K. Li, J. Solid State Chem. 183 (2010) 1221–1225.
[17] M. He, L. Kienle, A. Simon, X.L. Chen, V. Duppel, J. Solid State Chem. 177 (2004) 3212–3218.
[18] M. He, X. Chen, H. Okudera, A. Simon, Chem. Mater. 17 (2005) 2193–2196.
[19] Y. Yue, Z. Wu, Z. Lin, Z. Hu, Solid State Sci. 13 (2011) 1172–1175.
[20] J.L. Kissick, D.A. Keszler, Acta Crystallogr. E 58 (2002) 85–87.
[21] R.D. Shannon, C.T. Prewitt, Acta Crystallogr. B 25 (5) (1969) 925–946.
[22] J.W. Visser, J. Appl. Crystallogr. 2 (1969) 89–95.
[23] Z.-G. Hu, T. Higashiyama, M. Yoshimura, Y. Mori, T. Sasaki, Z. Kristallog. NCS 214 (1999) 433–434.
[24] L.A. Solovyov, J. Appl. Cryst. 37 (2004) 743–749.
[25] S.K. Kurtz, T.T. Perry, J. Appl. Phys. 39 (8) (1968) 3798–3813.
[26] T.C. Ozawa, S.J. Kang, J. Appl. Cryst. 37 (2004) 679.
[27] R.W. Smith, M.A. Kennard, M.J. Dudik, Mater. Res. Bull. 32 (6) (1997) 649–656.
[28] J.A. Kaduk, L.C. Satek, S.T. McKenna, Rigaku J. 16 (2) (1999) 17–30.
[29] A.S. Korotkov, V.V. Atuchin, Opt. Commun. 281 (2008) 2132–2138.
[30] A.S. Korotkov, V.V. Atuchin, J. Phys. Chem. Solids 71 (7) (2010) 958–964.